

Cellulose Carbon-CVD Carbon Composites

S. Marinkovic*, P. W. Whang, A. Navarrete and P. L. Walker, Jr.

Reprinted from TANSO 1976 (No. 84)

Cellulose Carbon-CVD Carbon Composites

S. Marinkovic*, P. W. Whang, A. Navarrete and P. L. Walker, Jr.

Department of Material Sciences
The Pennsylvania State University
University Park, Pennsylvania 16802

(Received June 10, 1975)

Carbon-carbon composites have been fabricated using a cellulose powder which is molded at low pressures, carbonized at 800°C and infiltrated by a CVD technique at 700°C using propylene as a source of carbon. Infiltration rate at time t is governed by the amount of open porosity existing in the sample at this time. These composites are then treated at temperatures ranging from 1000°C to 2400°C. Flexural strength, elastic modulus, Knoop hardness and electrical conductivity of the composites are progressively changed with increasing apparent density (d), following expressions of the type $Y = ad^b$. Coefficient of thermal expansion, wear resistance and oxidation resistance increase with infiltration time, while surface area sharply drops to a low value after initial infiltration. Heat treatment (HT) of the composites considerably changes their properties, but not monotonically with increasing HTT. Rather they show maxima or minima at 1500–2000°C HTT. However, property-density relationships of the same type (but with different constants a and b) as for non-heat-treated samples are generally preserved after HT. Comparison of the densest composites with corresponding commercial glassy carbons heat treated to similar temperatures shows that oxidation rate and coefficient of thermal expansion of the composites are lower, flexural strength and electrical conductivity are similar, while Young's modulus, wear resistance and hardness are greater for the glassy carbons.

1. INTRODUCTION

Carbon-carbon composites are of increasing interest particularly for aerospace applications. The most common approach at producing these materials is to infiltrate woven carbon fiber structures by the chemical vapor deposition (CVD) of carbon from a hydrocarbon gas. Such an approach has been reviewed in detail by Kotlensky (1). Alternatively, compacted carbon particles which are more or less weakly bonded together can serve as a substrate for the addition of carbon by chemical vapor deposition. In this study porous cellulose carbon artifacts fabricated from micron-sized cellulose powder served as the substrate for the production of carbon-carbon composites. Cellulose has the virtue for this application of having a low carbon yield upon carbonization (about 18% by weight). Hence, an artifact of high open porosity can be produced which lends itself to large additions of a second phase — like CVD carbon.

2. EXPERIMENTAL

2.1 Preparation of Uninfiltrated Artifacts

Cellulose powder obtained from Applied Science Laboratory, Inc. has been used as a starting material. The powder had a particle size range from 2 to 27 μ with a maximum in the distribution at 12 μ . From water adsorption measurements, it is estimated to have a crystallinity of 74% by weight (2).

In order to establish optimum conditions for the fabrication of cellulose carbon artifacts to be used as substrates for CVD infiltration, an extensive study of the influence of molding pressure and heating cycle on properties of artifacts was made. Bars 5 cm long by 0.50 cm wide by 0.45 cm thick were prepared, using molding pressures ranging from 175 to 3500 kg/cm². These bars were initially cured and carbonized under conditions previously reported (3). These experiments have shown that closed porosity is increased and open porosity is reduced with increasing molding pressure. That is, with an increase in molding pressure from 175 to 3500 kg/cm² open porosity decreased from 57.1% to 6.7% while closed porosity increased from 12.0% to 30.1%. Apparent density of the artifacts increased from

* Present Address, Boris Kidric Institute, Belgrade, Yugoslavia.

0.68 g/cc to 1.39 g/cc. The theoretical infiltration density (TID) calculated according to Kotlensky, assuming a density of 2.1 g/cc for the CVD carbon, would increase from 1.47 g/cc for artifacts prepared at 3500 kg/cm² to 1.85 g/cc for artifacts prepared at the lowest molding pressure. A molding pressure of 210 kg/cm² selected for the preparation of all samples to be reported on.

Experiments were directed to establish effects of curing temperature and heating rate up to the maximum temperature (800°C) on the quality of the artifacts produced. Samples were packed in carbon black and heated under 1 atm of N₂. Upon heating to 800°C, the cellulose powder undergoes a weight loss of about 82%. However, most of this weight loss occurs during the primary degradation process which starts at about 250°C. The most critical part of the thermal cycle involves allowing an extended curing time at about 250°C. If this was not done, substantial bending and cracking of the samples occurred. The cycle standardized upon was: heating to 150°C at a rate of 2°C/min, then at 1.4°C/min to 250°C, curing for 20 hr at 250°C, heating at 1.7°C/min to 300°C, at 2.4°C/min to 500°C, at 4.5°C/min to 800°C, and finally soaking at 800°C for 1 hr. The total elapsed time for the curing and heating cycle was 30 hr.

2.2 Infiltration Conditions

A 50% propylene-50% helium mixture was used at atmospheric pressure for infiltration. On the basis of a number of experiments, 700°C was chosen as a desirable infiltration temperature. At this temperature samples were infiltrated for 72 hr without any noticeable external surface deposition. Higher temperatures lead to an increased surface deposition and formation of an impervious coating before the porous body is filled with carbon to the desired density.

The gas mixture passed in laminar flow through the reactor, it having a residence time of 4 min in the hot zone. Prior to its introduction, it was dried by passage over P₂O₅ and CaCl₂. In order to rapidly establish the desired gas composition in the unit when commencing a deposition run, the entire system was evacuated of helium (used during heat up) prior to introduction of the propylene-helium mixture. A three zone furnace was employed to obtain a hot zone 18 cm long and 7.5 cm in diameter in which the temperature could be maintained within ±2°C. Up to twenty samples could be infiltrated at one time.

2.3 Heat Treatment Procedure

Some samples infiltrated at 700°C were further heat treated to higher temperatures under 1 atm of helium using a graphite resistance furnace. Samples were heated

to the desired temperature at a rate of 10°C/min and held at final temperature for 1 hr.

2.4 Measurement of Sample Properties

Densities were determined by several methods; apparent density from the weight and dimensions, mercury density by mercury displacement at a pressure of 1 atm, and in some selected cases, methanol density at 25°C using a pycnometer. Pore size distribution was measured by using a mercury porosimeter at pressures up to 1000 atm; which is equivalent to a pore diameter of 140Å.

Flexural strength was measured by a three-point bending test using the Instron universal testing machine, and Young's modulus from the resonant frequency of flexural vibration, using a Namette Company acoustic spectrometer. Knoop microhardness was determined by a Leitz miniload hardness tester. In order to make indentations more visible, the polished cross-sectional surface of the sample was coated prior to testing with a thin aluminum film (200Å).

Wear resistance was determined using a standard polishing machine. Samples with approximate planar dimensions of 9×3 mm were pressed by a 740 g load onto silicon carbide abrasive paper No. 320 located at a distance 2.5 cm from the center of the polishing disc. They were abraded using a fixed number of revolutions of the abrasive paper at a speed of 180 turns/min in flowing water. Weight loss per 500 revolutions was taken as a measure of wear resistance. For comparison, wear resistances of stainless steel (67 Fe-18 Ni-13 Cr-2 Mo), sintered alumina (density 3.84 g/cc), and Tokai glassy carbons were also measured.

Oxidation resistance was measured using a Fisher TGA apparatus. Samples were heated in a stream of N₂ up to a desired temperature (500°C for most samples and 600°C for the more oxidation resistant). After 15 min, during which the temperature stabilized, air was admitted at a rate of 200 cc/min. The weight of the sample was continuously recorded as a function of time until 70–80% of the initial weight was consumed. Curves of burn-off versus time were used to determine the maximum rate of oxidation, $R_T = -dw/w_0 dt$, where w_0 is the initial sample weight.

Interlayer spacing, $c/2$, and crystallite height, L_c , were determined by using an x-ray unit consisting of a Picker generator and Siemens goniometer. The $c/2$ was determined from the peak position and L_c from the width at half maximum of the (002) reflection recorded at a goniometer speed of 0.5°(2θ)/min using nickel-filtered copper radiation.

The coefficient of thermal expansion (CTE) in the

100–400°C temperature range was determined using a DuPont 942 Thermomechanical Analyzer. Electrical resistance was measured employing a potential probe method which utilized two extra electrodes to eliminate errors due to contact resistance.

Surface areas were determined from N_2 (77°K) and CO_2 (298°K) adsorption measurements using a volumetric-type apparatus. An equilibration time of 30 min was allowed for each adsorption point. Surface areas were calculated using the BET equation for N_2 and the Dubinin equation (4) for CO_2 . Molecular areas of $16.2A^2$ and $25.3A^2$ were taken for N_2 and CO_2 , respectively.

3. RESULTS AND DISCUSSION

3.1 Properties of Samples Infiltrated for Various Times

As a result of curing and carbonization, the dimension of the uninfiltrated samples decreased to 3.5 cm long, 0.37 cm wide, and 0.30 cm thick. This represents a volume shrinkage over the original compacted cellulose powder of 65%.

With increasing infiltration time, apparent density of the samples increased as their porosity decreased. It may be expected that for a given set of conditions the rate of infiltration at time t should be proportional to the open porosity (θ) present in the sample at that time. Hence

$$-\frac{d\theta}{dt} = k\theta, \quad (1)$$

where the rate of infiltration is expressed as the rate of decrease of open porosity. From equation (1) it follows that

$$\log \frac{\theta_t}{\theta_0} = -k't. \quad (2)$$

or, if the remaining open porosity at time t , θ_t , is expressed as a percentage of the initial porosity θ_0 ,

$$\log (100 \theta_t / \theta_0) = 2 - k't \quad (3)$$

A plot of $\log (100 \theta_t / \theta_0)$ vs time, shown in Figure 1, confirms the assumed linear relationship between $\log \theta_t$ and t (although the extrapolated straight line intersects the porosity axis at 1.95 instead of 2.0). The infiltration rate constant obtained from the slope equals -0.00877 hr^{-1} . For example, to reduce the open porosity by a factor of two, infiltration need last about 34 hr. It should be emphasized that open porosity was taken as that in voids down to 140A, i.e., the size filled by mercury at 1000 atm pressure. Close agreement between mercury and methanol densities indicated that the amount of open porosity present in voids less than 140A in diameter in the artifact was small.

Figure 2 shows that the open porosity decreases

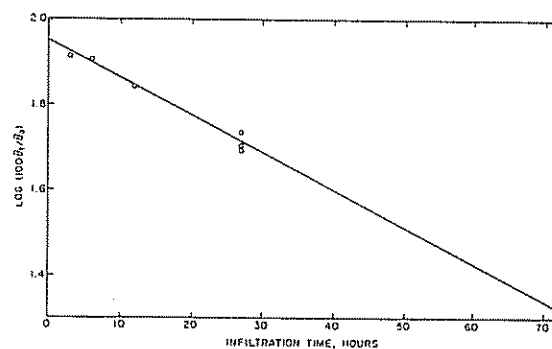


Fig. 1 Change of open porosity expressed as percent of initial open porosity with time of infiltration of cellulose carbon artifacts.

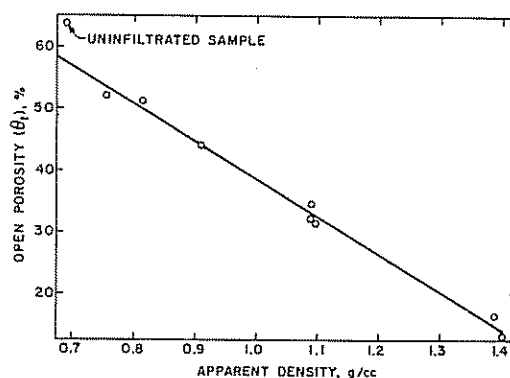


Fig. 2 Change of open porosity with change in apparent density of cellulose carbon artifacts as a result of carbon infiltration.

linearly with increasing apparent density of the infiltrated samples, following an initial sharp decrease in porosity at low infiltration levels. From the maximum density of the infiltrated artifacts, as found by extrapolating the straight line to $\theta_t = 0$ and from the fact that there is a negligible change in volume of the artifacts, the CVD carbon is estimated to have an apparent density of 1.64 g/cc.

Changes in flexural strength (σ), Young's modulus (E), Knoop hardness (H), and electrical resistivity (ρ) with changes in apparent density of the artifacts upon infiltration can be expressed by log-log plots, as seen in Figure 3. In all cases experimental points fit linear plots reasonably well, except for the uninfiltrated sample. The deviation is particularly high in the case of microhardness, which sharply decreases after the initial infiltration and then increases linearly. In going from the uninfiltrated samples to the samples infiltrated for the longest time (72 hr), properties change as follows: flexural strength increases from 100 to 800 kg/cm², Young's

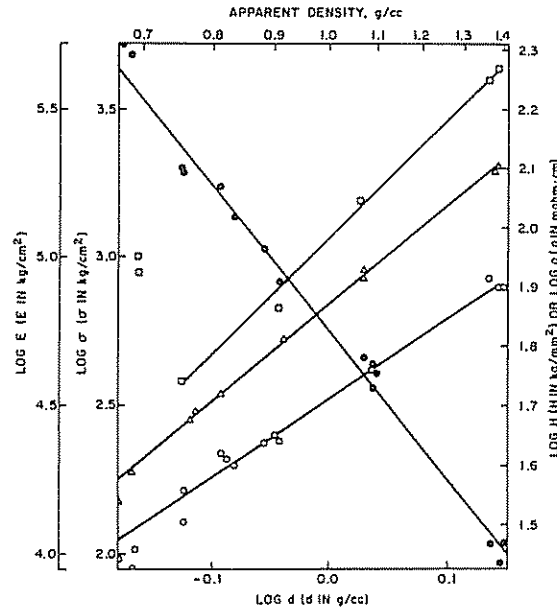


Fig. 3 Dependence of flexural strength (○), Young's modulus (△), Knoop hardness (□), and electrical resistivity (■) upon apparent density of composites.

modulus increases from 1.7×10^4 to 2.0×10^5 kg/cm², Knoop hardness increases from 86 to 182 kg/mm², and electrical resistivity decreases from 200 to 29 mohm-cm.

In preliminary experiments directed at arriving at a suitable infiltration temperature, some infiltration runs were made at 810°C. This temperature produced a too rapid rate of carbon deposition, resulting in blocking of the pores at the exterior surface of the bars, and in an extensive increase in dimensions of the artifact as carbon built up on the surface. On selected samples, infiltrated for 24 hr at 810°C, flexural strength and Young's modulus were measured. Despite the infiltration increasing the apparent density of the artifact to 1.1 g/cc, the flexural strength was essentially unchanged from the value for the uninfiltrated sample, 100 kg/cm², much less than 430 kg/cm² for the artifact infiltrated at 700°C to a density of 1.1 g/cc. In contrast, infiltration at 700 or 810°C produced similar values of Young's modulus. Experience gained throughout the program has led to the conclusion that whenever a surface coating appears on the artifact (either due to an increased infiltration temperature or to an extended deposition time), reduction in strength is always observed.

The coefficient of thermal expansion increases with increasing infiltration time (or apparent density) as seen in Table 1. Kotlensky summarizes available CTE data

Table 1 Wear resistance and CTE of infiltrated samples treated at different temperature

Infiltration time, hr	HTT °C	Wear mg/500 revol.	CTE × 10 ⁶ °C ⁻¹
0	No HT	—	1.35
12	No HT	1940	1.52
24	No HT	240	—
72	No HT	3.0	2.53
0	1000	—	0.90
12	1000	804	1.24
24	1000	273	—
72	1000	4.7	2.08
0	1500	—	0.51
12	1500	1012	—
24	1500	400	—
72	1500	8.7	1.39
24	2000	1170	—
72	2000	65	1.39
72	2400	190	1.39

for infiltrated felts and woven samples, and shows that there is a wide variation with raw materials and processing conditions (1). As seen in Table 1, infiltration with CVD carbon markedly improves the wear resistance of the base cellulose carbon. Following infiltration for 72 hr, it wears less rapidly than the stainless steel sample which loses 17.7 mg in 500 revolutions. However, the most fully infiltrated sample still has a wear resistance inferior to alumina (0.60 mg in 500 revolutions).

The x-ray diffraction profile of the cellulose carbon was very diffuse and did not permit an estimate of interlayer spacing or crystallite size. A better defined (002) reflection was observed following infiltration for 72 hr, from which the CVD carbon is estimated to have $c/2$ of 3.54Å and an L_c of 15Å.

Figure 4 presents reactivity results in air at 500°C. Infiltration of the base cellulose carbon markedly reduces reactivity. In the region of constant (and maximum) oxidation rate, reactivities are 4.1% burn-off/min for the original artifact, 1.4%/min following infiltration

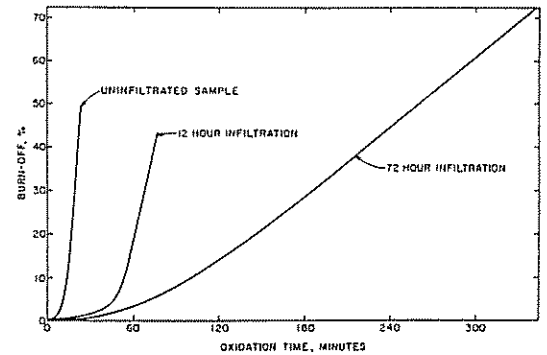


Fig. 4 Reactivity of composites to air at 500°C.

with CVD carbon for 12 hr, and 0.27%/min following infiltration for 72 hr. It was possible to follow controlled oxidation out to a burn-off level of 70% on the sample infiltrated 72 hr before spontaneous ignition occurred. On the other two samples, at a burn-off of about 45% spontaneous ignition occurred and the temperature increased in an uncontrolled manner.

The uninfiltreated carbon artifacts have high specific surface areas, that is, areas in CO_2 and N_2 are 1050 and $480 \text{ m}^2/\text{g}$. A difference in these areas is indicative of some molecular sieving in pores between 4 and 5A (5). As expected, infiltration for only 3 hr sharply reduces the CO_2 and N_2 areas to 16 and $4 \text{ m}^2/\text{g}$. Further infiltration does not have a major effect on specific surface areas.

3.2 Effect of Heat Treatment on Properties of Composites

Samples were heat treated at temperatures of 1000, 1500, 2000, and 2400°C. Figure 5 summarizes results on changes in weight, linear dimension and sample density with heat treatment temperature (HTT). It is seen that if the cellulose carbon artifacts are taken to 800°C and if CVD infiltration with propylene is carried out at 700°C, subsequent heat treatment up to 2400°C produces relatively little changes in sample weight and dimensions. Changes in dimensions which do occur can be associated primarily with two factors – shrinkage because of crystallite growth and alignment, and expansion because of relaxation of residual stresses and pressure build-up of gases in closed pores.

Table 2 summarizes x-ray diffraction results for both uninfiltreated samples and those infiltrated for 72 hr, followed by heat treatment up to 2400°C. For the uninfiltreated samples, crystallite growth is small, and three dimensional layer plane alignment is negligible for heat treatment up to 2400°C. This is expected for cellulose carbon. For the infiltrated samples, on the other hand, significant crystallite growth of the CVD carbon occurs. Further, interlayer spacing monotonically decreases with increasing HTT such that at 2400°C the spacing indicates significant planar alignment into an ababab registry (6).

Changes in flexural strength, Young's modulus, Knoop hardness and electrical resistivity with increasing HTT for the uninfiltreated samples and those infiltrated at 700°C for 3, 24, and 72 hr were studied. Heat treatment has relatively little effect on flexural strength or Young's modulus for artifacts infiltrated up to 24 hr. For the 72 hr infiltrated samples, flexural strength goes through a pronounced maximum at about 1500°C HTT and then decreases with further heat treatment. This behavior is

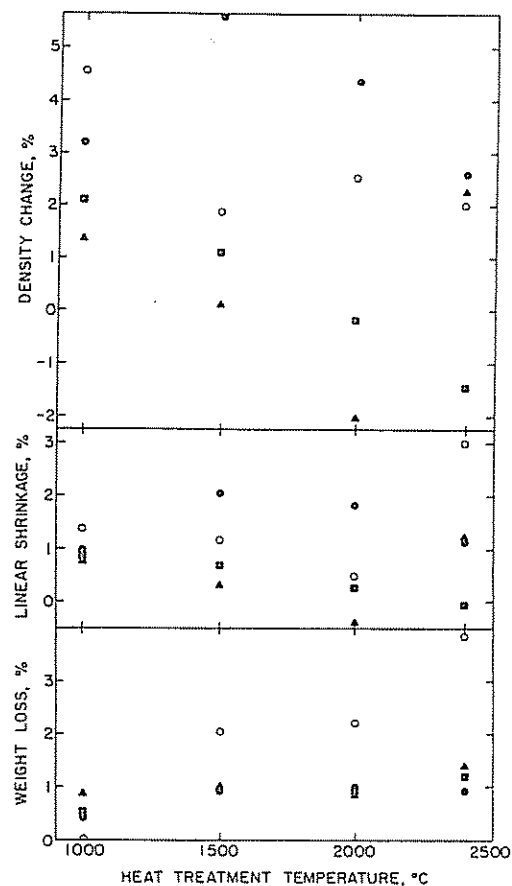


Fig. 5 Weight loss, linear shrinkage, and density change upon heat treatment of composites produced by carbon infiltration for varying times: 0, no infiltration; \blacktriangle , 3 hr; \blacksquare , 12 hr; \bullet , 72 hr.

Table 2 Interlayer spacing and L_c for uninfiltreated and 72 hr infiltrated samples

Sample	HTT, °C	Interlayer Spacing, Å	L_c , Å
U	None	Too diffuse	—
I	None	3.54	15
U	1000	3.79	11
I	1000	3.53	16
U	1500	3.65	13
I	1500	3.50	38
U	2000	3.57	16
I	2000	3.465	94
U	2400	3.435	40
I	2400	3.383	125

analogous to the change of density with HTT. Young's modulus of the 72 hr infiltrated samples goes through a shallow maximum following heat treatment at 1000°C and then decreases continually with further increases in

HTT. Knoop hardness of the uninfiltreated samples monotonically decreases with increasing HTT. For the infiltrated samples, hardnesses go through maxima with increasing HTT. In each case, however, the hardness of the composites heated to 2400°C is substantially lower than the hardness of the unheat-treated samples.

Electrical resistivities decrease sharply with increasing HTT. Most of the decrease occurs with heat treatment up to 1500°C and is primarily attributed to removal of hetero-atoms from carbon atoms located at the periphery of small trigonally bonded crystallites (7). The result is the production of positive hole carriers. Heat treatment above 1500°C results in little further decrease in resistivity since increase in crystallite size produces two counter-balancing effects – an increase in carrier mobility but a decrease in number of positive hole carriers.

As is the case for the unheat-treated composites (Figure 3), log-log plots of σ , E , and H versus composite density give straight lines for each HTT. Therefore, log-log plots of E vs σ give straight lines for each HTT, with the slope of the plots decreasing with increasing HTT. Although log-log plots of ρ versus density are also linear at lower HTT, they become increasingly curved (concave) as HTT is increased.

Heat treatment of the 72 hr infiltrated composite to 1500 or 2000°C markedly reduces reactivity to air over that found for the non-heat-treated sample (Figure 4). Reactivity of the 1500°C heat-treated sample was measured at 500°C; whereas because of its very low reactivity, the sample having a HTT of 2000°C was oxidized at 600°C. Decreases in reactivity with increasing HTT generally are attributed to one or more of the following

reasons: decrease in active surface area, increase in crystallinity, and decrease in amount of impurities which can act as oxidation catalysts. In this case for the infiltrated samples, CO₂ surface areas, in fact, increased upon heat treatment to 1500°C. However, as discussed previously (8), an increase in total surface area as given by CO₂ adsorption does not necessarily mean that the surface area active to oxidation would also increase. X-ray diffraction studies of some samples following oxidation at 500°C to large burn-offs showed that the carbon remaining had a lower mean interlayer spacing and larger average crystallite height than that contained in the original carbon composites. This is in agreement with previous studies on the gasification of electrode graphite composites (9), that is the less crystalline material is being reacted away preferentially.

It is of interest to compare the properties of the carbon-carbon composites prepared in this study with the properties of commercial glassy carbons. In Table 3 properties are compared for the 72 hr infiltrated composites with those of Tokai glassy carbons GC-10, 20, and 30 heat treated at 1000, 2000, and 3000°C. Densities of the composites are slightly lower than for the glassy carbons; in both cases they change little with HTT. Open porosities of the carbon composites are significantly higher than those in the glassy carbons; however, open porosities in the glassy carbons increase sharply with increasing HTT. At comparable HTT, oxidation rates of the glassy carbons are higher than those for the carbon composites. For both materials oxidation rates decrease sharply with increasing HTT. In the case of the glassy carbons this may be due primarily to a decrease in ash content with increasing HTT.

Table 3 Comparison of properties for 72 hour infiltrated samples with those of Tokai glassy carbons

Material	Apparent Density g/cc	Open Porosity %	Maximum Oxidation Rate, % Burn-off/min	Flexural Strength kg/cm ²	Young's Modulus kg/mm ²	CTE ^b × 10 ⁶ °C ⁻¹	Electrical Resistivity mohm-cm	Wear mg/500 Revol.	Hardness kg/mm ²
<u>Infiltrated Samples</u>									
No HT	1.39	11.5	0.27 ^c	820	2000	2.5	28	3.0	186
1000°C	1.43	13.9	0.13 ^c	940	2150	2.1	10	4.7	205
1500°C	1.46	12.8	0.028 ^c	1250	1950	1.4	7.2	8.7	173
2000°C	1.45	12.9	0.143 ^d	1250	1800	1.4	7.2	65	128
2400°C	1.43	13.6	0.046 ^d	1070	1550	1.4	7.1	190	110
<u>Tokai Samples^a</u>									
GC-10	1.48–1.51	0.2–0.4	(0.060) ^c	(830–935)	3000–3300	2.0–2.2	(11)	(1.4)	(273)
GC-20	1.47–1.50	1–3	(0.245) ^d	(925)	3000–3300	2.0–2.2	(8.3)	(1.5)	(234)
GC-30	1.44–1.47	3–5	(0.081) ^d	500–600	2200–2500	2.0–2.2	3.5–4.0	(10.5)	(154)

^a Values were taken from reference (10); values in parentheses were determined by the authors

^b For the interval 100–400°C (composites) or at 100°C (Tokai)

^c Measured at 500°C

^d Measured at 600°C

That is, in going from GC-10 to GC-30 the ash content is reported to drop from >1000 ppm to <100 ppm (10). At comparable HHT flexural strengths of the two carbons are similar, but Young's moduli of the glassy carbons are significantly higher. Whereas the CTE of the carbons for a HTT of 1000°C are comparable, the carbon composites have lower CTE values for treatment above 2000°C. For comparable HTT, electrical resistivities of the two carbons are similar. Wear resistance of both materials is seen to decrease with increasing HTT, but at comparable HTT the wear resistance of the glassy carbons is much superior to the carbon composites. The same situation holds for Knoop hardness values.

Glassy (and vitreous) carbons have found a number of metallurgical and mechanical applications as boats, crucibles, seals, and susceptors. It is interesting to speculate as to whether carbon composites as prepared in this study also have some applications in this field. It is expected that the total time required to produce the composites will be significantly less than that required to produce the glassy carbons because of the very long curing and carbonization cycle required in the latter case.

4. CONCLUSIONS

Cellulose powder can be compacted at room temperature into artifacts which upon curing and carbonization lead to bodies of low density (0.68 g/cc) and large open porosities (64%). In turn, the open porosity in these bodies can be filled by the deposit of carbon from the cracking of a hydrocarbon to produce a composite of higher density, increased strength and modulus, increased wear resistance and hardness, increased oxidation resistance, and decreased electrical resistivity. The infiltration rate at time t is governed by the open porosity (θ_t) at this time, whence the equation $\theta_t = \theta_0 \exp(-k't)$. A number of properties (Y) are related to the apparent

density (d) of the artifact by the equation $Y = ad^b$ where values of a and b are functions of the particular property and HTT. Some properties of the composites produced using a long infiltration time (72 hr) are superior to those of commercial glassy carbons for comparable HTT (for example, oxidation resistance); whereas other properties are inferior (such as wear resistance).

Acknowledgements

This study was supported by the Advanced Research Projects Agency on Contract No. DAH15 71 C 0290. The cellulose powder was kindly supplied gratis by Applied Science Laboratories, Inc., State College, Pennsylvania.

REFERENCES

1. Kotlensky, W. V., Chemistry and Physics of Carbon, (P. L. Walker, Jr. and P. A. Thrower, Editors), Vol. 9, Marcel Dekker, New York, 1973, p. 173.
2. Christner, L. G., Ph.D. Thesis, The Pennsylvania State University, 1972.
3. Nagle, D. C. and Walker, P. L., Jr., Extended Abstracts, Eleventh Biennial Conference on Carbon, 1973, p. 322.
4. Dubinin, M. M., Chemistry and Physics of Carbon, (P. L. Walker, Jr., Editor), Vol. 2, Marcel Dekker, New York, 1966, p. 51.
5. Walker, P. L., Jr., Austin, L. G., and Nandi, S. P., *ibid.*, p. 257.
6. Franklin, R. E., *Acta Cryst.*, 3, 107 (1950).
7. Pinnick, H. T., Proceedings of the Conferences on Carbon, University of Buffalo, 1956, p. 3.
8. Laine, N. R., Vastola, F. J., and Walker, P. L., Jr., *J. Phys. Chem.*, 67, 2030 (1963).
9. Walker, P. L., Jr., McKinstry, H. A., and Wright, C. C., *Ind. Eng. Chem.*, 45, 1711 (1953).
10. Yamada, S., Report 68-2, Defense Ceramic Information Center, Battelle Memorial Institute, 1968.

要 旨

セルローズカーボンとCVDカーボンとの複合体

低圧でセルローズ粉末をモールド成形して800°Cに炭化させた材料に、プロピレンを700°Cで浸透、CVD処理(Chemical Vapor Deposition)して作った複合体を1000~2400°C間の種々の温度で熱処理した。浸透速度はその度の開いた多孔度に支配された。曲げ強さ、弾性率、クヌーブ硬度、電気比抵抗は、試料の見掛密度 d と、 $Y = a \cdot d^b$ という関係にあった。熱膨脹係数(CTE)、耐摩耗性、耐酸化性は浸透時間と共に増加し、表面積は

浸透初期に急に減少した。熱処理温度は、試料の特性を大きく変化させたが、処理温度上昇と共に単純増加又は減少することはなかった。比較のために、最密のものとしてのglassy carbon製品を測定した結果、CTEや酸化速度は、この複合体の方が低く、曲げ強さや比抵抗は相似、弾性率、耐摩耗性、硬度はglassy carbonの方が大きかった。